Geophysical Research Letters

Key Points:
- No amount of salt is sufficient to cause basal melting of south polar ice on Mars under typical conditions
- Under an ideal composition of an ice-perchlorate mixture, basal melting may occur if the geothermal heat flux is >72 mW m^{-2}
- A subsurface magma chamber may provide sufficient heat for local, transient melting of basal polar ice

Correspondence to:
M. M. Sori and A. M. Bramson,
michael.sori@gmail.com;
bramson@lpl.arizona.edu

Water on Mars, With a Grain of Salt: Local Heat Anomalies Are Required for Basal Melting of Ice at the South Pole Today

Michael M. Sori[1] (iD) **and Ali M. Bramson[1]** (iD)

[1]Lunar and Planetary Laboratory, University of Arizona, Tucson, AZ, USA

Abstract Recent analysis of radar data from the Mars Express spacecraft has interpreted bright subsurface radar reflections as indicators of local liquid water at the base of the south polar layered deposits (SPLD). However, the physical and geological conditions required to produce melting at this location were not quantified. Here we use thermophysical models to constrain parameters necessary to generate liquid water beneath the SPLD. We show that no concentration of salt is sufficient to melt ice at the base of the SPLD in the present day under typical Martian conditions. Instead, a local enhancement in the geothermal heat flux of >72 mW/m^2 is required, even under the most favorable compositional considerations. This heat flow is most simply achieved via the presence of a subsurface magma chamber emplaced 100 s of kyr ago. Thus, if the liquid water interpretation of the observations is correct, magmatism on Mars may have been active extremely recently.

Plain Language Summary Recent radar observations from the European Space Agency's Mars Express spacecraft have been interpreted as evidence for melting beneath the ice at the south pole of Mars. We model the temperatures in the subsurface to determine the necessary conditions to achieve liquid water at the base of the ice cap. Salts lower the melting point of ice, with calcium-perchlorate generating the lowest temperatures at which melting can be achieved. However, even if there are local concentrations of large amounts of these salts at the base of the south polar ice, typical Martian conditions are too cold to melt the ice. We find that a local heat source within the crust is needed to increase the temperatures, and a magma chamber within 10 km of the ice could provide such a heat source. This result suggests that if the liquid water interpretation of the observations is correct, magmatism on Mars may have been active extremely recently.

1. Introduction

The prevalence, stability, and timing of liquid water on Mars have profound importance for the geology, geomorphology, and astrobiological potential of the planet. However, liquid water at the present day is not stable at the surface under expected typical Martian conditions (e.g., Haberle et al., 2001). Special circumstances, however, like lava-ice interactions, could have generated transient liquid water in the Amazonian period (the last ~3 Gyr). One way to generate liquid water may be through basal melting of subglacial ice. This explanation has been suggested for a proposed midlatitude esker (Butcher et al., 2017). At the present day, this effect is most likely to occur beneath the thick north polar layered deposits (NPLD) and south polar layered deposits (SPLD), if the chemistry and geothermal heat at the base of the kilometers-thick ice deposits is sufficient to cause melting (Clifford, 1987; Fisher et al., 2010; Wieczorek, 2008). Such polar basal melting was possibly important in Mars' ancient hydrological cycle (e.g., Baker et al., 1991; Fastook et al., 2012; Head & Pratt, 2001), but whether it can occur today is ambiguous.

One way to investigate evidence for subsurface melting is with MARSIS (Mars Advanced Radar for Subsurface and Ionosphere Sounding), a radar sounder onboard the European Space Agency's Mars Express spacecraft (Picardi et al., 2005). This low-frequency radar has a 1-MHz bandwidth that can operate in four bands centered on 1.8, 3.0, 4.0, and 5.0 MHz and is capable of penetrating kilometers into the subsurface. In 29 raw data tracks taken by MARSIS over the SPLD, Orosei et al. (2018) found a zone centered at 193°E, 81°S in which the basal reflectors appear anomalously bright when normalized to the power of the surface echo. They concluded that these bright basal reflectors are due to a material with dielectric permittivity >15, which they interpret as an indication of the presence of liquid water in this location. Orosei et al. (2018) suggest that the presence of salts (particularly perchlorates), which lower the freezing point of the ice

and could lead to either a sludge within the soils or localized brine pools, offers an explanation for their liquid water interpretation. Salts could be atmospherically sourced, and experiments suggest Na-perchlorates may be the most efficient ice nucleating particle available on Mars (Santiago-Materese et al., 2018). These salts could be concentrated in the subsurface, as seen at the Phoenix landing site (Cull et al., 2010), to create an impermeable crust. Proposed mechanisms for concentrating salts include migration of thin films of liquid water (Cull et al., 2010) and repeated episodes of sublimation when the units currently at the bottom of the SPLD were near the surface (Head & Marchant, 2014). However, a detailed quantitative model of the salt concentration and geothermal heat flux necessary for basal melting was not performed, leaving it unclear if the liquid water interpretation mandates implausible physical constraints.

In this paper, we assume the interpretation of anomalous radar returns as subglacial liquid water (Orosei et al., 2018) is correct and then quantify the necessary conditions to melt ice at that location. Previous work has estimated some of the necessary physical parameters to generate such an effect in the polar regions (Clifford, 1987; Fisher et al., 2010; Wieczorek, 2008), and here we build on those studies by simultaneously considering salt content, heat flow, and temperature-dependent thermal conductivities. We use thermal models to constrain the salt content, geothermal heat flux, and dust content necessary to produce basal melting at the SPLD. We consider the geological history necessary to produce the required conditions for basal melting of the SPLD and discuss implications for the liquid water interpretation of Orosei et al. (2018).

2. Methods

The central method we use is an application of Fourier's law of thermal conduction:

$$Q = -k\nabla T, \tag{1}$$

where T is temperature, Q is the local heat flux, and k is thermal conductivity, which can be both depth and temperature dependent. Our goal is to produce a large enough thermal gradient such that the base of the SPLD reaches the melting point of ice ("ice" refers to H_2O ice in this paper unless otherwise noted). The free parameters we consider are Q and the percentage and type of perchlorate in the ice, which will affect the melting point. The temperature at the top of the SPLD is derived using a thermal model, described below. We consider an SPLD thickness of 1.5 km, consistent with that observed at the location of the proposed liquid water (Orosei et al., 2018), and assume the SPLD is a mixture of ice and dust, which affects the thermal conductivity. Specific considerations for the melting point, surface temperature, and thermal conductivity are described below.

Salts can depress the melting point of ice, and in the polar regions of Mars, perchlorates are important to consider, as Mg, Na, and Ca perchlorates were detected at high latitudes by the Wet Chemistry Laboratory on the Phoenix Mars Lander (Hecht et al., 2009). For Mg and Ca perchlorate, we use the melting temperature in a perchlorate-H_2O mixture as measured in laboratory experiments (Pestova et al., 2005). For Na perchlorate, we consider the melting temperature in a perchlorate-H_2O mixture predicted by theoretical calculations (Chevrier et al., 2009). Note that only some of the mixture is required to be liquid in order to be consistent with the radar evidence (Orosei et al., 2018). Perchlorates can cause H_2O melting at temperatures as low as 236 K for Na, as low as 205 K for Mg, and as low as 199 K for Ca. We calculate a lower limit on the heat flux Q required to cause basal melting, and to do so we assume that any perchlorates are concentrated at the base of the SPLD (having perchlorates distributed throughout the SPLD would only allow for a small concentration in order to not violate density constraints of the whole SPLD (Wieczorek, 2008; Zuber et al., 2007).

We used a one-dimensional (1-D) thermal conduction model to calculate the annual average surface temperature of the SPLD, a necessary parameter in our application of Fourier's law. This model uses a semi-implicit Crank-Nicolson numerical method (Crank & Nicolson, 1947) to simulate a surface energy balance that accounts for insolation, blackbody radiation, and thermal conduction within subsurface layers for present-day orbital and rotational parameters of Mars. We use 15 numerical layers within one diurnal skin depth and increase layer thickness by 3% until the bottom layer reaches a depth of six annual skin depths, a scheme that sufficiently resolves diurnal and annual thermal variations. We solve the thermal diffusion

equation at the boundaries of each numerical subsurface layer. The modeled surface is flat, consistent with the SPLD surface above the putative liquid water (Orosei et al., 2018), and we assume the surface has an albedo of 0.4 and an infrared emissivity of 0.9. However, when the surface temperature drops below the frost point of carbon dioxide (~150 K), frost condenses on the surface, fixing the surface temperature to the frost point; during these periods, we use an albedo of CO_2 frost of 0.7 and emissivity of 0.7 instead. We consider the presence of a low-conductivity surficial layer (e.g., a sublimation lag deposit or dust coating a ~meter thick), with cohesive, high-conductivity ice underneath (see following paragraph for the parameters considered for each layer). We calculate the temperature at every layer boundary in 100-s intervals throughout one Mars year, yielding an annual-average surface temperature at 81°S (the latitude of the putative liquid water (Orosei et al., 2018) of 162 K for a nominal geothermal heat flux of 30 mW/m². Varying the geothermal heat flux in the lower boundary condition between 0–200 mW/m² only changes the annual average surface temperature by <0.2 K. Our thermal model yields robust temperature results across the solar system (Sori et al., 2017, 2018), including for Mars (Bramson et al., 2017; Hamilton et al., 2018), and the annual average surface temperature that we use here (162 K) is consistent with those modeled by others (e.g., Mellon et al., 2004).

The thermal conductivity k throughout the SPLD controls the temperature-depth profile once the surface temperature is calculated and a heat flux is chosen. We allow k to vary with depth. In the upper meter, we assume a low thermal conductivity unit ($k = 0.02$ W·m^{-1}·K^{-1}), based on observations of low thermal inertias in the Mars south polar region (Putzig et al., 2005). The low thermal inertia layer (180 J·m^{-2}·s$^{-0.5}$·K^{-1}) serves to insulate the underlying SPLD, raising the temperature by a few Kelvin compared to the case where the surface unit is cohesive, high-conductivity ice. This stratigraphic model allows us to set a minimum constraint on the geothermal heat flux required to cause basal melting, as the absence of such a low-conductivity surface layer would require a higher heat flux to sufficiently raise basal temperature. For the rest of the 1.5-km column of the SPLD, we assume an ice-dust mixture with the higher thermal conductivities associated with cohesive units.

We assume the conductivity of the mixture is the volumetrically weighted average of ice and dust. The composition of dust is assumed to have $k = 2$ W·m^{-1}·K^{-1}, and ice is assumed to have a temperature-dependent $k = 651/T$, where T is the temperature of the ice at that depth (Petrenko & Whitworth, 1999). Because perchlorates are assumed to be concentrated at the base of the SPLD (see above), their presence does not affect the thermal conductivity of the 1.5-km-thick ice-dust column in our model. Gravity inversions yield a best fit dust content for the SPLD as a whole of ~15% by volume, but uncertainties are large and allow for pure ice (Wieczorek, 2008; Zuber et al., 2007). Analysis of the propagation of MARSIS signals implies the SPLD has between 0% and 10% dust (Plaut et al., 2007). We nominally consider dust contents of 0% and 20% uniformly mixed through the SPLD, which yield lower and upper constraints, respectively, on basal temperature. We additionally consider cases where the dust is concentrated in specific layers. We note that previous work assumed a uniform value for k that was temperature independent (Clifford, 1987; Fisher et al., 2010). This approximation is allowable for those studies because they assumed a heat flux of 30 mW/m², but we will show that for the higher heat fluxes required to melt basal ice, temperature-dependent effects and the role of dust become nontrivial.

We use the 1-dimensional version of equation (1) to calculate temperature profiles with depth. The top of the profile is set to the annual average surface temperature of 162 K calculated from our semi-implicit thermal conduction model. We calculate the temperature at depth in steps of 1 m throughout the 1,500-m vertical profile. At each spatial step, the thermal conductivity is calculated using the temperature in the previous (i.e., above) step, which is used as an input to equation (1) to calculate the temperature. At a depth of 1,500 m, the basal temperature is compared to various melting points.

3. Results

Figure 1a shows temperature-depth profiles for heat fluxes of $Q = 10$, 30, and 90 mW/m², and for compositions of pure ice and 80% ice/20% dust. Temperature profiles are compared to the melting point of ice, for both pure ice and perchlorate salt mixtures at the base. The inclusion of 20% dust in the SPLD raises the basal temperature by <1 K for the 10 mW/m² case, but by 5 K for the 90 mW/m² case. Additionally, using a temperature-dependent thermal conductivity increases the basal temperature by <1 K for the
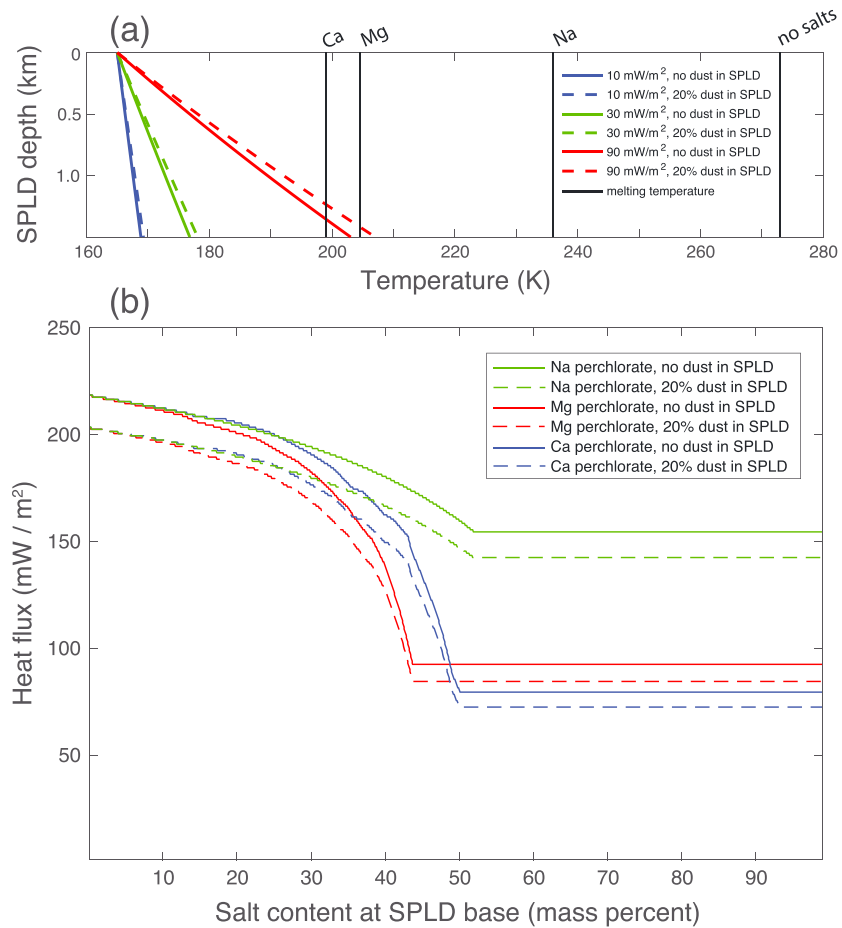
Figure 1. (a) Simulated temperature-depth profiles in the south polar layered deposits (SPLD) at the location where basal liquid water has been proposed, for geothermal heat fluxes of 10 (blue), 30 (green), and 90 (red) mW/m^2 and dust contents of 0% (solid lines) and 20% (dashed lines). All profiles consider temperature-dependent thermal conductivity. Vertical lines represent the eutectic temperature for Ca, Mg, and Na perchlorate-ice mixtures and the melting temperature for pure ice (no salts). (b) Minimum geothermal heat fluxes required to reach the liquidus (or temperature for a liquid water-salt crystal mixture for salt contents greater than the eutectic content) as a function of salt content in the ice.

10 mW/m^2 case compared to that of a strictly linear thermal gradient with depth, and by 5 K for the 90 mW/m^2 case.

The SPLD and NPLD exhibit layering at a variety of spatial scales, which have been attributed to variable concentrations of ice and dust due to climatic variations while the deposits have been growing (e.g., Becerra et al., 2017; Cutts & Lewis, 1982; Laskar et al., 2002). We investigated the effect that the distribution of dust within the SPLD has on the temperature-depth profile. In the most extreme case of having all of the 20% of dust concentrated into a single non-icy layer near the top of the SPLD, the basal temperature is ~3 K greater compared to uniform mixing for a heat flux of 90 mW/m^2. Such a structure is not physically plausible for the SPLD but serves as an end-member case to show the maximum possible effect of layering, and results shown hereafter assume uniform mixing of dust, for cases when it is present.

We calculate temperature-depth profiles for heat fluxes ranging from 1 to 250 mW/m^2 in increments of 1 mW/m^2 for cases of pure ice and 80% ice/20% dust. In each case, we record the basal temperature and compare it to the freezing point for an ice-salt mixture. We consider Mg, Ca, and Na perchlorates, with mass percentages ranging from 0% to 99% in increments of 1%. For each comparison, we record whether the temperature-depth profile reaches a basal temperature greater than the freezing point. Some of these

AGU
100
ADVANCING EARTH
AND SPACE SCIENCE

Geophysical Research Letters

10.1029/2018GL080985

temperature-depth profiles are shown in Figure 1a; full results for basal temperatures for all parameters considered can be found in the supporting information.

The minimum geothermal heat fluxes required for reaching the liquidus for a given salt content are shown in Figure 1b. A heat flux of 72 mW/m^2 is required for basal melting of H$_2$O under the most favorable conditions of 50% or more Ca perchlorate by mass at the base of the SPLD and an SPLD that contains the maximum estimated quantities of dust (20% by volume). Lower concentrations of perchlorate yield less melt. If the SPLD has a volumetrically negligible amount of dust mixed into the ice instead, a heat flux of 80 mW/m^2 is required. These numbers change if the perchlorate has a different chemistry. For Mg perchlorate, the minimum heat fluxes under 20% dust and 0% dust are 85 and 93 mW/m^2, respectively, and for Na perchlorate, they are 143 and 155 mW/m^2, respectively. If no perchlorate is present, heat fluxes of 204 and 219 mW/m^2 are required for cases of 20% and 0% dust, respectively.

4. Discussion

Under the most favorable compositions, a geothermal heat flux of $Q = 72$ mW/m^2 is required to melt ice and generate liquid water at the location proposed by recent radar analysis (Orosei et al., 2018). Is this heat flux possible under normal conditions on Mars? A commonly used value (e.g., Clifford, 1987; Fisher et al., 2010) for Q is 30 mW/m^2, a number which assumes heat production comes from a Mars with bulk chondritic composition (Fanale, 1976). However, more recent analysis that considers the loading of the polar deposits suggests that Mars is subchondritic with respect to heat-producing elements (Phillips et al., 2008). When this result is combined with maps of crustal thickness, a global average value of $Q = 19$ mW/m^2 is instead inferred, with regional variations ranging from 14 to 25 mW/m^2 (Parro et al., 2017). These estimates will be verified or revised with direct observations from NASA's InSight mission (Spohn et al., 2014), but it is difficult to imagine the measured Q will be a factor of 4 times greater or more than current estimates. It is therefore highly unlikely that the necessary $Q > 72$ mW/m^2 could be achieved under typical conditions on Mars today.

Localized enhancements of heat flux under ice sheets may be possible under special geological conditions. On Earth, high geothermal heat fluxes of >200 mW/m^2 have been observed beneath the Antarctic ice sheet (Fisher et al., 2015; Schroeder et al., 2014), much greater than the average terrestrial value. A variety of geological processes and structures can contribute to geothermal heat flow (e.g., Rezvanbehbahani et al., 2017). However, most of these factors are either already accounted for in the models that predict Mars' low geothermal heat flux (such as crustal thickness) or are not applicable to Mars (such as factors related to plate tectonics). Models of Martian midlatitude glaciation similarly found that increases in geothermal heat flux were needed to achieve subglacial melting but also required strain heating of the ice due to internal deformation of flowing ice (Butcher et al., 2017). This effect is not observed to be occurring in the polar layered deposits (Karlsson et al., 2011), nor is it predicted to occur except possibly at some margins (Sori et al., 2016). A local concentration of heat-producing elements in the crust may increase the geothermal heat flux, but not by the magnitude required (e.g., Laneuville et al., 2013).

One set of processes that could plausibly lead to elevated heat flow are volcanic or magmatic processes. We quantify the magmatic activity that would be required to generate $Q > 72$ mW/m^2 on Mars today using 2-D finite element method modeling that solves the two-dimensional version of equation (1). We consider cases where a circular magma chamber at temperature 1,300 K and diameter D is buried at depth H beneath the SPLD in the Martian crust (Figure 2a). We assume the magma chamber is directly beneath the 1.5 km of SPLD that is proposed to overlay liquid water. We mesh a domain with nodes every 100 m for a 50 km by 50 km grid and numerically solve the heat equation at each element, assuming the upper boundary of the domain (i.e., bottom of the ice) is at 199 K (the lowest melting point for any perchlorate mixture we investigated; see Figure 1a). We assume the crust has thermal conductivity $k = 2$ W·m^{-1}·K^{-1}, background heat flux 30 mW/m^2, specific heat capacity $c = 800$ J·kg^{-1}·K^{-1}, and density of 2,500 kg/m^3. The model steps forward in time, quantifying how heat diffuses, and we record the heat flux at the top of the domain at each time step. This finite element method approach is similar to previous work that quantified heat flux below Martian shield volcanoes (Fassett & Head, 2006).
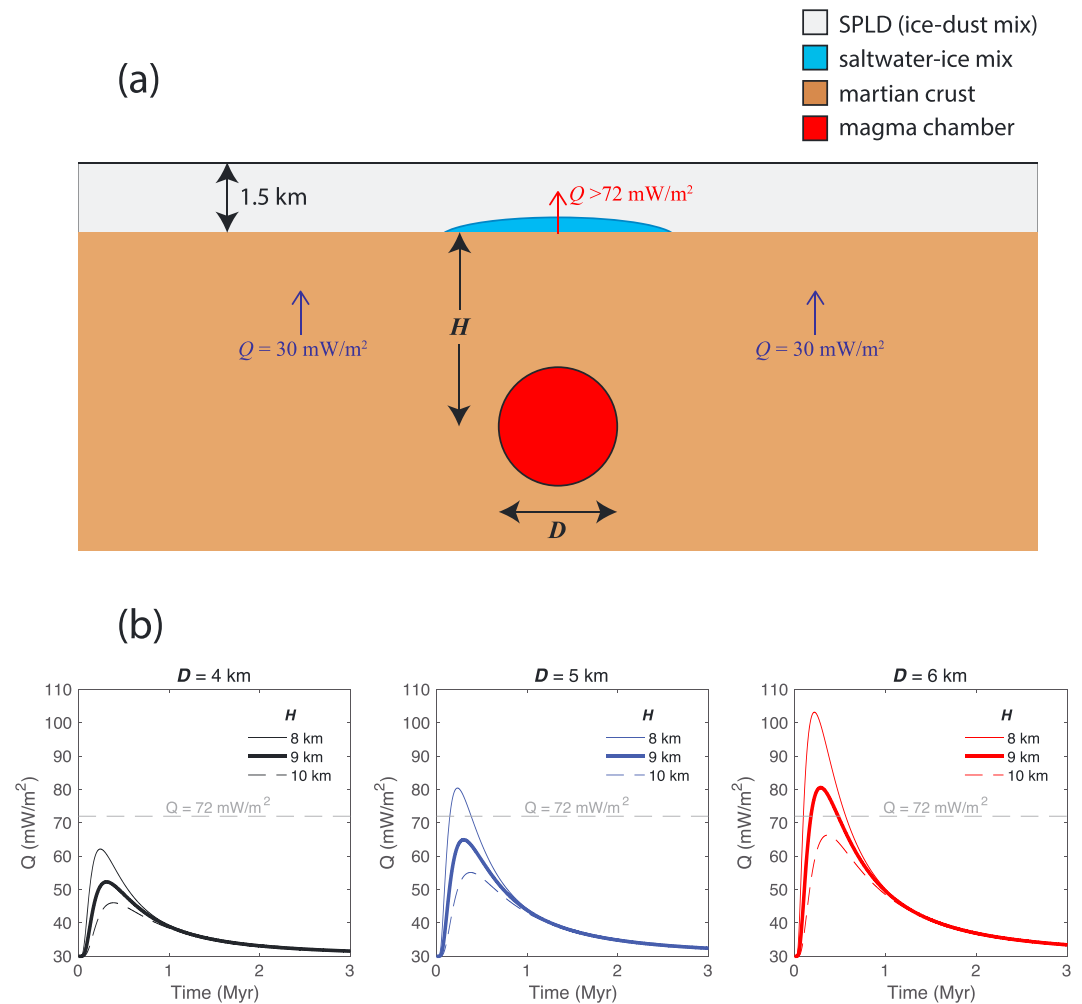
Figure 2. (a) Schematic of the case we consider causing a local elevated heat flux beneath the south polar layered deposits (SPLD): (a) magma chamber of diameter D is buried a depth H (to the center of the chamber) beneath the putative liquid water, creating an elevated heat flux Q as it cools. The background geothermal heat flux is set to 30 mW/m^2. (b) Finite element method results showing the heat flux at the SPLD-crust interface at the location of the putative liquid water, as a function of D and H.

We find that a magma chamber at a depth of 8 km would need to have a diameter of >5 km in order to produce a heat flux that reaches >72 mW/m^2 at the base of the ice (Figure 2b). The size of the magma chamber required increases with depth to the magma chamber; for example, for a magma chamber at a depth of 9 km, a diameter of >6 km is needed. The size of the magma chamber is a lower limit, as the background heat flux of 30 mW/m^2 is likely an overestimate (Parro et al., 2017; Phillips et al., 2008), and the required heat flux of 72 mW/m^2 assumes ideal basal composition of perchlorates. The maximum heat flux is reached ~300 kyr after emplacement of the magma chamber, decreasing to the background heat flux after ~2 Myr. According to estimates of magma production rates on Mars (Greeley & Schneid, 1991), the necessary volume of magma could be emplaced in 750 years or more.

There is mineralogical evidence of subglacial volcanic activity in the south polar region (Ackiss et al., 2018), although this activity likely occurred in the pre-Amazonian era. However, crater size-frequency analysis has revealed volcanic units that formed in the late Amazonian era elsewhere on Mars (e.g., Hamilton et al., 2010), including features that may be 5 Myr old (Jaeger et al., 2010) or younger (Garvin et al., 2000; Horvath & Andrews-Hanna, 2018). Additionally, meteoritic analysis supports the occurrence of magmatism in the Amazonian period (Udry & Day, 2018). These observations are not directly connected to the potential magmatic activity we quantify here but serve to show that Mars may still experience ongoing igneous

activity. A depth of ~10 km to the center of a magma chamber on Mars is also reasonable (Wilson & Head, 1994). Thus, the model results lead us to conclude that recent magmatism may offer a plausible explanation for enhanced heat flux. Gravity inversions intriguingly suggest a positive density anomaly near the region, which could be associated with subsurface structure in the crust involving magmatism (Li et al., 2012), but future higher-resolution gravity data would be needed to convincingly test this possible association.

The calculations above assume some perchlorates are present to facilitate melting at relatively low temperatures. As an end-member case, we also consider what size of magma chamber would achieve geothermal heat fluxes in excess of 204 mW/m^2, the minimum flux required to achieve basal melting of ice in the absence of any perchlorates. This heat flux could be achieved with a magma chamber emplaced ~100 kyr ago several kilometers closer to the surface (depth to the center of the magma chamber being on a similar scale as its diameter, i.e., $H < 6$ km for $D = 6$ km or $H < 4.5$ km for $D = 4$ km). Thus, if magmatic intrusions can attain sufficiently shallow depths, it is not necessary to invoke salts to achieve basal melting.

The size and geometry of the subsurface magma chamber may have important lateral effects at the SPLD-crust interface. The area in which Orosei et al. (2018) detected anomalously high dielectric permittivity is ~20-km wide. If this area completely corresponds to an area of liquid water, our estimates of magma chamber size may be a lower constraint. Our models quantify the necessary parameters to generate water at a point above the magma chamber, rather than across an entire 20-km patch. If further analysis of the MARSIS radar data confirms the area of the region of high basal reflection power, then larger magma chamber sizes or other geometries, such as sills, may need to be invoked.

We identify two alternatives to the interpretation of local magmatism causing a local enhancement of geothermal heat flux at the base of the SPLD. The first is that our modeling of temperature profiles is incomplete, which is only important if the net result of missing effects is to increase basal temperature sufficiently to render our conclusion of a local enhancement of geothermal heat flux unnecessary. These effects, however, are likely to be very minor compared to the >25-K temperature increase that they would need to provide. The difference between the maximum inferred Q on Mars (25 mW/m^2) and the minimum required Q under the most favorable compositional conditions (72 mW/m^2) is large. The overburden pressure from the weight of the SPLD will slightly depress the melting point at the base, but we calculate this effect to be 0.3 K if the SPLD is pure ice and 0.5 K if the SPLD is 20% dust by volume (assuming ice density = 917 kg/m^3 and dust density = 2,500 kg/m^3). Relatively low-conductivity CO_2 ice deposits are present in parts of the SPLD subsurface but only comprise ~1% of the total SPLD volume and have not been confirmed in the area considered here (Bierson et al., 2016; Phillips et al., 2011; Putzig et al., 2018). The thermal conduction model we used (Bramson et al., 2017) to calculate the annual average surface temperature (162 K) considers a simplified atmosphere that parameterizes infrared and visible scattering, but not attenuation through the path length of the atmosphere, which is more important at the higher incidence angles in polar regions. Atmospheric attenuation, following the scheme provided in Schorghofer and Edgett (2006) and Aharonson and Schorghofer (2006), could lower the annual average surface temperature by ~5 K, which would increase the geothermal heat flux necessary for melting. Finally, obliquity variations could have a time-lagged effect on basal temperatures (Fisher et al., 2010), but this is likely to be a minor effect in the present day as obliquity variations have had a low amplitude over the past ~300 kyr (Laskar et al., 2002), and the time lag for penetration of thermal waves driven by obliquity changes occurs on order ~10 kyr. We therefore argue that the enhanced geothermal heat flux conclusion is robust if there is basal melting under the SPLD.

The second alternative to recent localized magmatism is the possibility that the radar data may be interpreted without liquid water and thus there is no need to invoke a high local geothermal heat flux. One important factor is that the MARSIS interpretations are model dependent; specifically, attenuation of the radar signal through the SPLD is temperature dependent. We show that for the expected range of typical geothermal heat flux on Mars today, the basal temperature of the SPLD is <180 K (Figure 1a). This relatively low temperature favors permittivity values on the lowest end of those inferred by the models of Orosei et al. (2018), which showed that warmer ice temperatures mandate higher dielectric constants to explain the same normalized basal echo power. Their modeling of radar attenuation through ice showed that the dielectric constant needed to generate the subsurface power returned may be ~15 for cold temperatures. In this case, the radar returns observed by Orosei et al. (2018) in this region would still represent a locality of anomalously high permittivity, but additional work will be necessary to determine the need to invoke wet

materials given that the models of the surrounding areas also include values as high as 15. Such work will be important for understanding not only the presence of liquid water on Mars today but also active magmatic processes, as we show here.

5. Conclusions

Basal melting of the SPLD at the location where liquid water has been proposed (Orosei et al., 2018) is not plausible under the typical geothermal heat fluxes expected of Mars, regardless of salt content. Basal melting instead (or additionally) requires a locally enhanced geothermal heat flux. For the most favorable compositional parameters (20% dust volume contained within the SPLD ice and Ca perchlorate concentrated at the base of the SPLD), a heat flux of $Q > 72$ mW/m^2 is required to create liquid water. Less idealized conditions lead to higher required heat fluxes; for example, the likelier case of nearly pure SPLD ice mandates $Q > 80$ mW/m^2 under the same basal salt content, or $Q > 93$ mW/m^2 if the perchlorate is Mg instead of Ca. We emphasize that these heat fluxes may be lower constraints depending on the fraction of melt required to generate the dielectric permittivity to explain the radar observations. With no salt content, $Q > 204$ mW/m^2 is required to achieve basal melting.

The necessary enhancement of heat flux may plausibly be achieved with the presence of a magma chamber in the subsurface. Under this scenario, the magma chamber must have been emplaced in the upper 10 km of the crust beneath the SPLD. Emplacement must have occurred 100 s of kyrs ago, due to the time lag for heat to conduct to the base of the SPLD. If the magma can attain depths of 5 km or less, it may be able to cause basal melting without any significant salt content in the ice. The magmatism explanation would imply that liquid water is unlikely to be widespread throughout the entire SPLD base, which is supported by the radar observations. Alternatively, it may be unnecessary to invoke liquid water at the base of the SPLD in order to interpret the MARSIS data, as the colder temperatures we calculate here would alter models of radar attenuation and may imply lower basal permittivity of the anomalous region. Additional work to confirm the interpretation of the radar data will be important for assessing the likelihood of basal melting and thus active magmatism on Mars today.

References

Ackiss, S., Horgan, B., Seelos, F., Farrand, W., & Wray, J. (2018). Mineralogic evidence for subglacial volcanism in the Sisyphi Montes region of Mars. *Icarus*, *311*, 357–370. https://doi.org/10.1016/j.icarus.2018.03.026

Aharonson, O., & Schorghofer, N. (2006). Subsurface ice on Mars with rough topography. *Journal of Geophysical Research*, *111*, E11007. https://doi.org/10.1029/2005JE002636

Baker, V. R., Strom, R. G., Gulick, V. C., Kargel, J. S., Komatsu, G., & Kale, V. S. (1991). Ancient oceans, ice sheets and the hydrological cycle on Mars. *Nature*, *352*(6336), 589–594. https://doi.org/10.1038/352589a0

Becerra, P., Sori, M. M., & Byrne, S. (2017). Signals of astronomical climate forcing in the exposure topography of the north polar layered deposits of Mars. *Geophysical Research Letters*, *44*, 62–70. https://doi.org/10.1002/2016GL071197

Bierson, C. J., Phillips, R. J., Smith, I. B., Wood, S. E., Putzig, N. E., Nunes, D., & Byrne, S. (2016). Stratigraphy and evolution of the buried CO$_2$ deposit in the Martian south polar cap. *Geophysical Research Letters*, *43*, 4172–4179. https://doi.org/10.1002/2016GL068457

Bramson, A. M., Byrne, S., & Bapst, J. (2017). Preservation of midlatitude ice sheets on Mars. *Journal of Geophysical Research: Planets*, *122*, 2250–2266. https://doi.org/10.1002/2017JE005357

Butcher, F. E. G., Balme, M. R., Gallagher, C., Arnold, N. S., Conway, S. J., Hagermann, A., & Lewis, S. R. (2017). Recent basal melting of a mid-latitude glacier on Mars. *Journal of Geophysical Research: Planets*, *122*, 2445–2468. https://doi.org/10.1002/2017JE005434

Chevrier, V. F., Hanley, J., & Altheide, T. S. (2009). Stability of perchlorate hydrates and their liquid solutions at the Phoenix landing site, Mars. *Geophysical Research Letters*, *36*, L10202. https://doi.org/10.1029/2009GL037497

Clifford, S. M. (1987). Polar basal melting on Mars. *Journal of Geophysical Research*, *92*(B9), 9135–9152. https://doi.org/10.1029/JB092iB09p09135

Crank, J., & Nicolson, P. (1947). A practical method for numerical evaluation of solutions of partial differential equations of the heat-conduction type. *Proceedings of the Cambridge Philosophical Society*, *43*(01), 50–67. https://doi.org/10.1017/S0305004100023197

Cull, S. C., Arvidson, R. E., Catalano, J. G., Ming, D. W., Morris, R. V., Mellon, M. T., & Lemmon, M. (2010). Concentrated perchlorate at the Mars Phoenix landing site: Evidence for thin film liquid water on Mars. *Geophysical Research Letters*, *37*, L22203. https://doi.org/10.1029/2010GL045269

Cutts, J. A., & Lewis, B. H. (1982). Models of climate cycles recorded in Martian polar layered deposits. *Icarus*, *50*(2-3), 216–244. https://doi.org/10.1016/0019-1035(82)90124-5

Fanale, F. P. (1976). Martian volatiles: Their degassing history and geochemical fate. *Icarus*, *28*(2), 179–202. https://doi.org/10.1016/0019-1035(76)90032-4

Fassett, C. I., & Head, J. W. (2006). Valleys on Hecates Tholus, Mars: Origin by basal melting of summit snowpack. *Planetary and Space Science*, *54*(4), 370–378. https://doi.org/10.1016/j.pss.2005.12.011

Fastook, J. L., Head, J. W., Marchant, D. R., Forget, F., & Madeleine, J.-B. (2012). Early Mars climate near the Noachian-Hesperian boundary: Independent evidence for cold conditions from basal melting of the south polar ice sheet (Dorsa Argentea Formation) and implications for valley network formation. *Icarus*, *219*(1), 25–40. https://doi.org/10.1016/j.icarus.2012.02.013

Fisher, A. T., Mankoff, K. D., Tulaczyk, S. M., Tyler, S. W., Foley, N., & the WISSARD Science Team (2015). High geothermal heat flux measured below the West Antarctic ice sheet. *Science Advances*, *1*(6), e1500093. https://doi.org/10.1126/sciadv.1500093

Fisher, D. A., Hecht, M. H., Kounaves, S. P., & Catling, D. C. (2010). A perchlorate brine lubricated deformable bed facilitating flow of the north polar cap of Mars: Possible mechanism for water table recharging. *Journal of Geophysical Research*, *115*, E00E12. https://doi.org/10.1029/2009JE003405

Garvin, J. B., Sakimoto, S. E. H., Frawley, J. J., Schnetzler, C. C., & Wright, H. M. (2000). Topographic evidence for geologically recent near-polar volcanism on Mars. *Icarus*, *145*(2), 648–652. https://doi.org/10.1006/icar.2000.6409

Greeley, R., & Schneid, B. D. (1991). Magma generation on Mars: Amounts, rates, and comparisons with Earth, Moon, and Venus. *Science*, *254*(5034), 996–998. https://doi.org/10.1126/science.254.5034.996

Haberle, R. M., McKay, C. P., Schaeffer, J., Cabrol, N. A., Grin, E. A., Zent, A. P., & Quinn, R. (2001). On the possibility of liquid water on present-day Mars. *Journal of Geophysical Research*, *106*(E10), 23,317–23,326. https://doi.org/10.1029/2000JE001360

Hamilton, C. W., Fagents, S. A., & Wilson, L. (2010). Geologic and thermodynamic constraints on the formation of the Tartarus Colles cone groups. *Journal of Geophysical Research*, *115*, E09006. https://doi.org/10.1029/2009JE003546

Hamilton, C. W., Mouginis-Mark, P. J., Sori, M. M., Scheidt, S. P., & Bramson, A. M. (2018). Episodes of aqueous flooding and effusive volcanism associated with Hrad Vallis, Mars. *Journal of Geophysical Research: Planets*, *123*, 1484–1510. https://doi.org/10.1029/2018JE005543

Head, J. W., & Marchant, D. R. (2014). The climate history of early Mars: Insights from the Antarctic McMurdo Dry Valleys hydrologic system. *Antarctic Science*, *26*(06), 774–800. https://doi.org/10.1017/S0954102014000686

Head, J. W., & Pratt, S. (2001). Extensive Hesperian-aged south polar ice sheet on Mars: Evidence for massive melting and retreat, and lateral flow and ponding of meltwater. *Journal of Geophysical Research*, *106*(E6), 12,275–12,299. https://doi.org/10.1029/2000JE001359

Hecht, M. H., Kounaves, S. P., Quinn, R. C., West, S. J., Young, S. M. M., Ming, D. W., et al. (2009). Detection of perchlorate and the soluble chemistry of martian soil at the Phoenix lander site. *Science*, *325*(5936), 64–67. https://doi.org/10.1126/science.1172466

Horvath, D. G., & Andrews-Hanna, J. C. (2018). The thickness and morphology of a young pyroclastic deposit in Cerberus Palus, Mars: Implications for the formation sequence, *Lunar Planet. Sci. Conf.* 49th, abstr. 2435.

Jaeger, W. L., Keszthelyi, L. P., Skinner, J. A. Jr., Milazzo, M. P., McEwen, A. S., Titus, T. N., et al. (2010). Emplacement of the youngest flood lava on Mars: A short, turbulent story. *Icarus*, *205*(1), 230–243. https://doi.org/10.1016/j.icarus.2009.09.011

Karlsson, N. B., Holt, J. W., & Hindmarsh, R. C. A. (2011). Testing for flow in the north polar layered deposits of Mars using radar stratigraphy and a simple 3D ice-flow model. *Geophysical Research Letters*, *38*, L24202. https://doi.org/10.1029/2011GL049630

Laneuville, M., Wieczorek, M. A., Breuer, D., & Tosi, N. (2013). Asymmetric thermal evolution of the Moon. *Journal of Geophysical Research: Planets*, *118*, 1435–1452. https://doi.org/10.1002/jgre.20103

Laskar, J., Levrard, B., & Mustard, J. F. (2002). Orbital forcing of the Martian polar layered deposits. *Nature*, *419*(6905), 375–377. https://doi.org/10.1038/nature01066

Li, J., Andrews-Hanna, J. C., Sun, Y., Phillips, R. J., Plaut, J. J., & Zuber, M. T. (2012). Density variations within the south polar layered deposits of Mars. *Journal of Geophysical Research*, *117*, E04006. https://doi.org/10.1029/2011JE003937

Mellon, M. T., Feldman, W. C., & Prettyman, T. H. (2004). The presence and stability of ground ice in the southern hemisphere of Mars. *Icarus*, *169*(2), 324–340. https://doi.org/10.1016/j.icarus.2003.10.022

Orosei, R., Lauro, S. E., Pettinelli, E., Cicchetti, A., Coradini, M., Cosciotti, B., et al. (2018). Radar evidence of subglacial liquid water on Mars. *Science 361*, 490–493, 6401. https://doi.org/10.1126/science.aar7268

Parro, L. M., Jiménez-Díaz, A., Mansilla, F., & Ruiz, J. (2017). Present-day heat flow model of Mars. *Nature Scientific Reports*, *7*(1), 45629. https://doi.org/10.1038/srep45629

Pestova, O. N., Myund, L. A., Khripun, M. K., & Prigaro, A. V. (2005). Polythermal study of the systems M (ClO$_4$)$_2$–H$_2$O (M^{2+} = Mg^{2+}, Ca^{2+}, Sr^{2+}, Ba^{2+}). *Russian Journal of Applied Chemistry*, *78*(3), 409–413. https://doi.org/10.1007/s11167-005-0306-z

Petrenko, V. F., & Whitworth, R. W. (1999). *Physics of ice*. Oxford, UK: Oxford University Press.

Phillips, R. J., Davis, B. J., Tanaka, K. L., Byrne, S., Mellon, M. T., Putzig, N. E., et al. (2011). Massive CO$_2$ ice deposits sequestered in the south polar layered deposits of Mars. *Science*, *332*(6031), 838–841. https://doi.org/10.1126/science.1203091

Phillips, R. J., Zuber, M. T., Smrekar, S. E., Mellon, M. T., Head, J. W., Tanaka, K. L., et al. (2008). Mars north polar deposits: Stratigraphy, age, and geodynamical response. *Science*, *320*(5880), 1182–1185. https://doi.org/10.1126/science.1157546

Picardi, G., Plaut, J. J., Biccari, D., Bombaci, O., Calabrese, D., Cartacci, M., et al. (2005). Radar soundings of the subsurface of Mars. *Science*, *310*(5756), 1925–1928. https://doi.org/10.1126/science.1122165

Plaut, J. J., Picardi, G., Safaeinili, A., Ivanov, A. B., Milkovich, S. M., Cicchetti, A., et al. (2007). Subsurface radar sounding of the south polar layered deposits of Mars. *Science*, *316*(5821), 92–95. https://doi.org/10.1126/science.1139672

Putzig, N. E., Mellon, M. T., Kretke, K. A., & Arvidson, R. E. (2005). Global thermal inertia and surface properties of Mars from the MGS mapping mission. *Icarus*, *173*(2), 325–341. https://doi.org/10.1016/j.icarus.2004.08.017

Putzig, N. E., Smith, I. B., Perry, M. R., Foss, F. J. II, Campbell, B. A., Phillips, R. J., & Seu, R. (2018). Three-dimensional radar imaging of structures and craters in the Martian polar caps. *Icarus*, *308*, 138–147. https://doi.org/10.1016/j.icarus.2017.09.023

Rezvanbehbahani, S., Stearns, L. A., Kadivar, A., Walker, J. D., & van der Veen, C. J. (2017). Predicting the geothermal heat flux in Greenland: A machine learning approach. *Geophysical Research Letters*, *44*, 12,271–12,279. https://doi.org/10.1002/2017GL075661

Santiago-Materese, D. L., Iraci, L. T., Clapham, M. E., & Chuang, P. Y. (2018). Chlorine-containing salts as water ice nucleating particles on Mars. *Icarus*, *202*, 280–287.

Schorghofer, N., & Edgett, K. S. (2006). Seasonal surface frost at low latitudes on Mars. *Icarus*, *180*(2), 321–334. https://doi.org/10.1016/j.icarus.2005.08.022

Schroeder, D. M., Blankenship, D. D., Young, D. A., & Quartini, E. (2014). Evidence for elevated and spatially variable geothermal flux beneath the West Antarctic ice sheet. *PNAS*, *111*(25), 9070–9072. https://doi.org/10.1073/pnas.1405184111

Sori, M. M., Bapst, J., Bramson, A. M., Byrne, S., & Landis, M. E. (2017). A Wunda-full world? Carbon dioxide ice deposits on Umbriel and other Uranian moons. *Icarus*, *290*, 1–13. https://doi.org/10.1016/j.icarus.2017.02.029

Sori, M. M., Byrne, S., Hamilton, C. W., & Landis, M. E. (2016). Viscous flow rates of icy topography on the north polar layered deposits of Mars. *Geophysical Research Letters*, *43*, 541–549. https://doi.org/10.1002/2015GL067298

Sori, M. M., Sizemore, H. G., Byrne, S., Bramson, A. M., Bland, M. T., Stein, N. T., & Russell, C. T. (2018). Cryovolcanic rates on Ceres revealed by topography. *Nature Astronomy*, *2*, 946–950. https://doi.org/10.1038/s41550-018-0574-1

Spohn, T., Grott, M., Smrekar, S., Krause, C., Hudson, T. L., & the HP^3 instrument team (2014). Measuring the Martian heat flow using the heat flow and physical properties package (HP^3), *Lunar Planet. Sci. Conf.* 45th, abstr. 1916.

Udry, A., & Day, J. M. D. (2018). 1.34 billion-year-old magmatism on Mars evaluated from the co-genetic nakhlite and chassignite meteorites. *Geochimica et Cosmochimica Acta*, *238*, 292–315. https://doi.org/10.1016/j.gca.2018.07.006

Wieczorek, M. A. (2008). Constraints on the composition of the Martian south polar cap from gravity and topography. *Icarus*, *196*(2), 506–517. https://doi.org/10.1016/j.icarus.2007.10.026

Wilson, L., & Head, J. W. (1994). Mars: Review and analysis of volcanic eruption theory and relationships to observed landforms. *Reviews of Geophysics*, *32*(3), 221–263. https://doi.org/10.1029/94RG01113

Zuber, M. T., Phillips, R. J., Andrews-Hanna, J. C., Asmar, S. W., Konopliv, A. S., Lemoine, F. G., et al. (2007). Density of Mars' south polar layered deposits. *Science*, *317*(5845), 1718–1719. https://doi.org/10.1126/science.1146995